

Coral oxygen isotope and in situ records capture the 2015/2016 El Niño event in the central equatorial Pacific

Gemma K. O'Connor¹, Kim M. Cobb², Hussein R Sayani², Alyssa R. Atwood³, Pamela R. Grothe², Samantha Stevenson⁴, Julia K Baum⁵, Tianran Chen⁶, Danielle Claar⁷, Nicholas Hitt⁸, Jean Lynch-Stieglitz², Gavin A. Schmidt⁹, and Rachel M. Walter²

¹University of Washington

²Georgia Institute of Technology

³Florida State University

⁴University of California, Santa Barbara

⁵University of Victoria

⁶South China Sea Institute of Oceanology

⁷Univ. of Victoria

⁸Victoria University Of Wellington

⁹NASA Goddard Institute for Space Studies

November 24, 2022

Abstract

Coral oxygen isotopes ($\delta^{18}\text{O}$) from the central equatorial Pacific provide monthly-resolved records of El Niño-Southern Oscillation (ENSO) activity over past centuries to millennia. However, calibration studies using in situ data to assess the relative contributions of warming and freshening to coral $\delta^{18}\text{O}$ records are exceedingly rare. Furthermore, the fidelity of coral $\delta^{18}\text{O}$ records under the most severe thermal stress events is difficult to assess. Here, we present six coral $\delta^{18}\text{O}$ records and in situ temperature, salinity, and seawater $\delta^{18}\text{O}$ data from Kiritimati Island (2°N, 15°W) spanning the very strong 2015/16 El Niño event. Local sea surface temperature (SST) anomalies of $+2.4 \pm 0.4^\circ\text{C}$ and seawater $\delta^{18}\text{O}$ anomalies of -0.19 ± 0.02 of -0.58 ± 0.05 from SST and $\sim 30\%$ from seawater $\delta^{18}\text{O}$. Our results demonstrate that Kiritimati coral $\delta^{18}\text{O}$ records can provide reliable reconstructions even during the largest class of El Niño events.

Hosted file

supplement_final.docx available at <https://authorea.com/users/548260/articles/603040-coral-oxygen-isotope-and-in-situ-records-capture-the-2015-2016-el-ni%C3%B1o-event-in-the-central-equatorial-pacific>

1 **Coral oxygen isotope and *in situ* records capture the 2015/2016**

2 **El Niño event in the central equatorial Pacific**

3
4 **Gemma K. O'Connor^{1,2}, Kim M. Cobb¹, Hussein R. Sayani¹, Alyssa T. Atwood³, Pamela R.**
5 **Grothe⁴, Samantha Stevenson⁵, Julia K. Baum⁶, Tianran Chen⁷, Danielle C. Claar^{6,8},**
6 **Nicholas T. Hitt⁹, Jean Lynch-Stieglitz¹, Gavin A. Schmidt¹⁰, Rachel Walter¹**

7 ¹School of Earth and Atmospheric Sciences, Georgia Institute of Technology, Atlanta, GA, USA

8 ²Department of Earth and Space Sciences, University of Washington, Seattle, WA, USA

9 ³Department of Earth, Ocean, and Atmospheric Science, Florida State University, Tallahassee,
10 FL, USA

11 ⁴Earth & Environmental Sciences, University of Mary Washington, Fredericksburg, VA, USA

12 ⁵Bren School of Environmental Science and Management, University of California-Santa
13 Barbara, Santa Barbara, CA, USA

14 ⁶Department of Biology, University of Victoria, Victoria, BC, Canada

15 ⁷South China Sea Institute of Oceanology, Chinese Academy of Sciences, Guangzhou, China

16 ⁸School of Aquatic and Fishery Sciences, University of Washington, Seattle, WA, USA

17 ⁹Victoria University of Wellington, Wellington, New Zealand

18 ¹⁰NASA Goddard Institute for Space Studies, New York, NY, USA

19 Corresponding author: Gemma K. O'Connor (goconnor@uw.edu)

20

21

22

23

24

25 **3 Key Points**

- 26 • An ensemble of coral oxygen isotope timeseries from the central equatorial Pacific tracks
27 the 2015/16 El Niño event.
- 28 • Coral oxygen isotope records reflect ~70% contribution from warming and ~30% from
29 freshening during the 2015/16 El Niño event.
- 30 • *In situ* seawater oxygen isotope data provide quantitative constraints on temperature
31 versus hydrological contributions to coral records.

32 **Abstract**

33 Coral oxygen isotopes ($\delta^{18}\text{O}$) from the central equatorial Pacific provide monthly-
34 resolved records of El Niño-Southern Oscillation (ENSO) activity over past centuries to
35 millennia. However, calibration studies using *in situ* data to assess the relative contributions of
36 warming and freshening to coral $\delta^{18}\text{O}$ records are exceedingly rare. Furthermore, the fidelity of
37 coral $\delta^{18}\text{O}$ records under the most severe thermal stress events is difficult to assess. Here, we
38 present six coral $\delta^{18}\text{O}$ records and *in situ* temperature, salinity, and seawater $\delta^{18}\text{O}$ data from
39 Kiritimati Island (2°N, 157°W) spanning the very strong 2015/16 El Niño event. Local sea
40 surface temperature (SST) anomalies of $+2.4\pm 0.4^\circ\text{C}$ and seawater $\delta^{18}\text{O}$ anomalies of -
41 $0.19\pm 0.02\text{‰}$ contribute to the observed coral $\delta^{18}\text{O}$ anomalies of $-0.58\pm 0.05\text{‰}$, consistent with a
42 ~70% contribution from SST and ~30% from seawater $\delta^{18}\text{O}$. Our results demonstrate that
43 Kiritimati coral $\delta^{18}\text{O}$ records can provide reliable reconstructions even during the largest class of
44 El Niño events.

45 **Plain Language Summary**

46 Oxygen isotope anomalies in coral skeletons provide reconstructions of year-to-year
47 ocean temperature variations in the tropical Pacific, which in turn have a profound influence on
48 global temperature and rainfall extremes. However, only a handful of calibrations exist that
49 quantify the relationship between ocean temperature and coral isotopic composition at a given
50 site, especially across extreme events where this relationship may vary most strongly. Here we
51 compare ocean temperature data from loggers installed on the reef at Kiritimati Island (2°N,
52 157°W) to coral oxygen isotopic records spanning the record-breaking 2015/16 El Niño event.
53 We find that the corals provide accurate reconstructions of ocean temperature extremes during
54 this very strong El Niño event, with ~70% of the signal originating from ocean temperature and
55 the remainder from increased rainfall.

56 **1 Introduction**

57 The El Niño/Southern Oscillation (ENSO) is the dominant mode of interannual climate
58 variability, but its response to greenhouse warming remains highly uncertain (Stevenson, 2012,
59 Bellenger et al., 2014, Ng et al., 2021). Although projections of ENSO-related SST variability
60 differ across climate models, simulations forced with projected anthropogenic greenhouse gas
61 emissions generally agree on an increase in the hydrological extremes associated with ENSO
62 (Power et al., 2013; Cai et al., 2014, Bonfils et al., 2015, Brown et al., 2020). This tendency
63 translates to an increase in the occurrence of ‘extreme’ El Niño events (as defined based on
64 equatorial Pacific precipitation) under continued greenhouse warming (Cai et al., 2015), although
65 models reflect a range of responses (Stevenson et al. 2021). Another question is whether
66 greenhouse gas-driven changes to ENSO have already taken place: observational studies of 20th
67 century ENSO extremes suggest a shift towards more Central Pacific warming events (Wang et
68 al., 2019), consistent with results from analysis of a large network of coral records spanning the

69 last several centuries (Freund et al., 2019). A number of paleoclimate ENSO reconstructions
70 document enhanced late 20th-century ENSO variability relative to the preindustrial era
71 (McGregor et al., 2013; Li et al., 2013; Cobb et al., 2013; Liu et al., 2017; Grothe et al., 2020),
72 supporting the idea that greenhouse warming has already led to a significant shift in ENSO
73 properties. However, it remains unclear how much of the observed shift in ENSO variance is due
74 to a strengthening of SST anomalies or hydrological extremes during ENSO events. This is
75 especially true for the largest trove of monthly-resolved ENSO reconstructions based on modern
76 and fossil corals from the central tropical Pacific, which documents a 25% increase in
77 interannual variability from the last millennia to the most recent decades (Grothe et al., 2020).

78 Oxygen isotope ratios ($\delta^{18}\text{O}$) in corals from the central tropical Pacific track ENSO-related
79 changes in SST and hydrology, with warmer and wetter conditions during El Niño events driving
80 negative coral $\delta^{18}\text{O}$ anomalies, while cool and dry conditions during La Niña events drive
81 positive coral $\delta^{18}\text{O}$ anomalies (Evans et al., 1999; Cobb et al., 2001; Nurhati et al., 2009). Cores
82 collected from living and fossil coral colonies have provided high-fidelity records of past ENSO
83 activity over recent decades (Cobb et al., 2001; Nurhati et al., 2009, 2011), centuries (Cobb et al.,
84 2003), and millennia (Cobb et al., 2013; McGregor et al., 2013; Grothe et al., 2020). The largest
85 such dataset comes from Kiritimati Island (2°N, 157°W), where ENSO dominates coral $\delta^{18}\text{O}$
86 variability as evidenced by correlation coefficients of ~ 0.80 between modern coral $\delta^{18}\text{O}$ records
87 and the NIÑO3.4 index (Grothe et al., 2020) - a key index of large-scale ENSO variability.

88 Despite their high-fidelity representation of instrumental SST variability over the satellite
89 era, coral $\delta^{18}\text{O}$ -based ENSO reconstructions are associated with a number of uncertainties. For
90 one, extremely high SSTs during strong El Niño events can induce thermal stress, which slows

91 or halts coral calcification, limiting the ability of coral proxies to capture the full extent of
92 temperature SST change during such events (e.g., Carilli et al., 2017). Indeed, previous coral
93 studies from the Eastern Pacific and Western Atlantic have found skeletal growth hiatuses during
94 very strong El Niño events (Dunbar et al., 1994), as well as systematic geochemical biases
95 initiated by extreme El Niño events (Hetzinger et al., 2016). Due to limited coral ensemble sizes
96 and *in situ* climate data, it remains unknown how well corals from the central tropical Pacific
97 record ENSO activity during extreme events. Second, coral $\delta^{18}\text{O}$ values reflect the combined
98 influence of SST and seawater $\delta^{18}\text{O}$ ($\delta^{18}\text{O}_{\text{sw}}$), but the relative contribution of SST vs. seawater
99 $\delta^{18}\text{O}$ to Kiritimati coral $\delta^{18}\text{O}$ records during ENSO extremes is difficult to assess without *in situ*
100 data. Previous work using paired Sr/Ca and coral $\delta^{18}\text{O}$ measurements showed a stronger than
101 normal $\delta^{18}\text{O}_{\text{sw}}$ contribution in Kiritimati coral $\delta^{18}\text{O}$ during the very strong 1997/98 El Niño event
102 (McGregor et al., 2013), but coverage among multiple strong events paired with *in situ* data is
103 needed to better understand these contributions. In particular, there are no systematic surveys of
104 seawater $\delta^{18}\text{O}$ variations across El Niño events, even though such variability has been inferred
105 from both models and observational data (Fairbanks et al., 1997, Russon et al., 2013, Conroy et
106 al., 2014).

107 In this study, we present six new coral $\delta^{18}\text{O}$ records as well as *in situ* records of SST,
108 salinity, and $\delta^{18}\text{O}_{\text{sw}}$ from Kiritimati Island spanning the 2015/16 El Niño event, one of the
109 strongest El Niño events on record. These data allow us to quantify the oceanographic changes
110 that occurred across this event, and their contribution to the observed coral $\delta^{18}\text{O}$ anomalies. By
111 comparing our results from the 2015/16 El Niño event to available coral $\delta^{18}\text{O}$ records and *in situ*
112 SST, salinity, and $\delta^{18}\text{O}_{\text{sw}}$ data from Kiritimati across past strong El Niño events of the 20th

113 century, we assess the stability of the relationship between SST, $\delta^{18}\text{O}_{\text{sw}}$, and coral $\delta^{18}\text{O}$ across
114 different El Niño events. This assessment is key to improving interpretation of coral $\delta^{18}\text{O}$ records
115 from the region.

116 **2 Methods**

117 Six modern coral cores from *Porites* spp. were recovered from a leeward open ocean reef flat
118 ranging from 20-30 ft depth (labelled “drill site” on Figure S1) at Kiritimati Island during
119 expeditions in April and November 2016. The cores were prepared and analyzed for coral $\delta^{18}\text{O}$
120 composition using standard procedures (Sayani et al., 2019, see Supplement for X-rays) on either
121 a Thermo-Finnigan Delta V or MAT253, both equipped with a Kiel IV Carbonate Device, with
122 analytical precisions of $\pm 0.05\text{‰}$ (1σ) and $\pm 0.06\text{‰}$ (1σ), respectively. Age models for each
123 record were reconstructed by peak matching the coral $\delta^{18}\text{O}$ data with $1^\circ \times 1^\circ$ monthly NOAA
124 OISSTv2 SST data (Reynolds et al., 2002) from the grid box containing Kiritimati Island,
125 following procedures outlined in Cobb (2002). Each record covers the 2015/16 El Niño event
126 and extends back 3-9 years prior to the event, depending on core length. Following Sayani et al.
127 (2019), we apply offsets of up to 0.19‰ to each record to align them to a common ensemble
128 mean (see Supplement).

129 We also present *in situ* SST, salinity, and $\delta^{18}\text{O}_{\text{sw}}$ data spanning the 2015/16 El Niño event
130 from Kiritimati Island. We present continuous time series of SST from a Seabird SBE56
131 temperature logger (Site 5 logger), and SST and salinity from a Seabird SBE37 conductivity-
132 temperature-depth (CTD) sensor (see Figure S1 for locations). We present 97 paired salinity and
133 $\delta^{18}\text{O}_{\text{sw}}$ data from seawater samples collected during field expeditions to Kiritimati Island from
134 2014 to 2016, and ~30 paired salinity and $\delta^{18}\text{O}_{\text{sw}}$ samples collected on the RV Moana Wave

135 from October to November, 1997. We include two *in situ* SST logger datasets from Kiritimati
136 Island presented by Claar et al., 2019 in our analyses: the first from the drill site, where corals in
137 this study were collected, and the second from a southward-facing reef flat several kilometers
138 away (Figure S1). We also use data from three gridded SST products, using the grid point closest
139 to Kiritimati Island: 1°x1° weekly OISSTv2, 1°x1° monthly HadISSTv1.1 (Rayner et al., 2003),
140 and 2°x2° monthly ERSSTv5 (Huang et al., 2017).

141

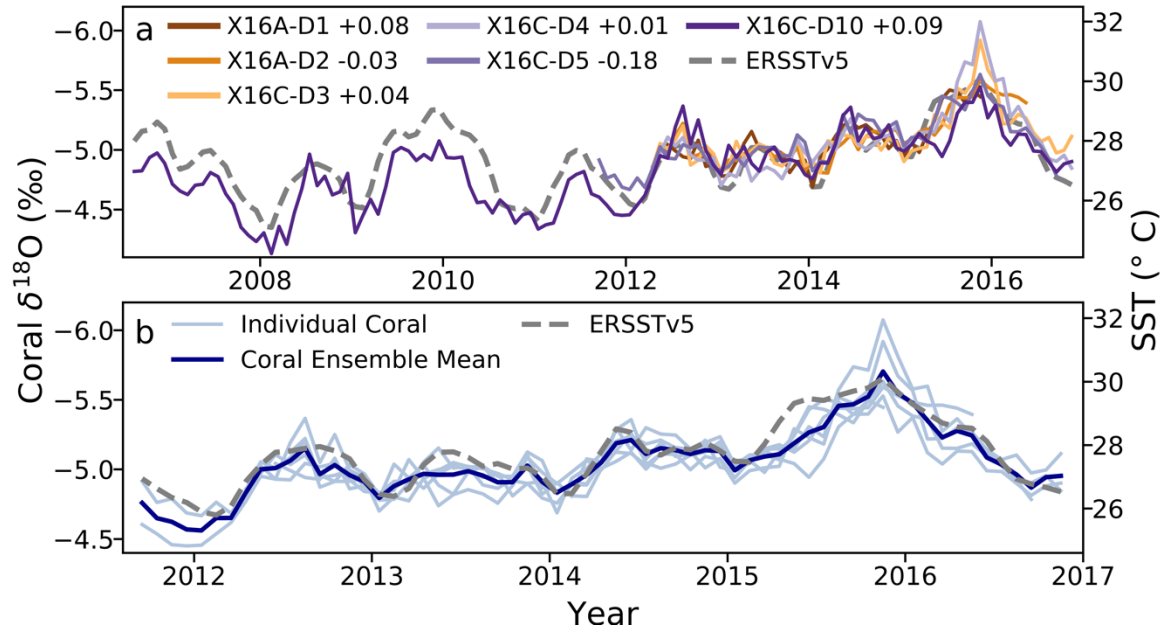
142 **3 Results**

143 **3.1 Coral $\delta^{18}\text{O}$ records**

144 All six coral $\delta^{18}\text{O}$ records closely follow instrumental SST and are highly reproducible on
145 monthly to annual timescales (Figure 1). Most of the variability in coral $\delta^{18}\text{O}$ is driven by ENSO,
146 as seasonal SST variability at this site is relatively small. The records are well correlated with
147 ERSSTv5, HadISST, and OISSTv2 (R between -0.81 and -0.91, $p < 0.05$, Table S8). A composite
148 coral $\delta^{18}\text{O}$ record formed by averaging overlapping records has a greater correlation with these
149 SST products than any individual record (R ~ -0.93; Figure 1b, Table S8). All coral $\delta^{18}\text{O}$ records
150 demonstrate consistent monthly variability across the study period, with correlations among
151 records ranging between 0.64 and 0.90 ($p < 0.05$). The 1σ spread in coral $\delta^{18}\text{O}$ values during any
152 given month of overlapping coral $\delta^{18}\text{O}$ records ranges from 0.04‰ to 0.24‰, with the maximum
153 variance occurring in November 2015, during the peak of the 2015/16 El Niño event.

154 During the 3-month peak of the event (October 2015 to December 2015), all six coral records
155 exhibit significant coral $\delta^{18}\text{O}$ depletion (mean of $-5.59 \pm 0.05\text{‰}$ (1SE)) coinciding with warmer
156 and fresher conditions. For the two-year baseline preceding the El Niño event (from January
157 2013 to January 2015, ending 9 months prior to the 3-month peak), the coral $\delta^{18}\text{O}$ records exhibit

158 a mean isotopic value of $-5.01 \pm 0.02\text{‰}$ (1 standard error (1SE)), reflecting a change in coral
 159 $\delta^{18}\text{O}$ of $-0.58 \pm 0.05\text{‰}$ (1SE).
 160



161
 162
 163 **Figure 1.** Coral $\delta^{18}\text{O}$ records (colored lines) from Kiritimati Island plotted with monthly
 164 resolved ERSSTv5 (gray dashed line) at Kiritimati Island (note inverted y-axis for coral $\delta^{18}\text{O}$).
 165 (a) New modern coral $\delta^{18}\text{O}$ records spanning the 2015/16 El Niño event as presented in this
 166 study. (b) Same as in (a), but with the ensemble mean of the corals shown. Coral $\delta^{18}\text{O}$ offsets
 167 have been applied (Supplement) and are denoted in the legend in panel (a) in units of per mil.

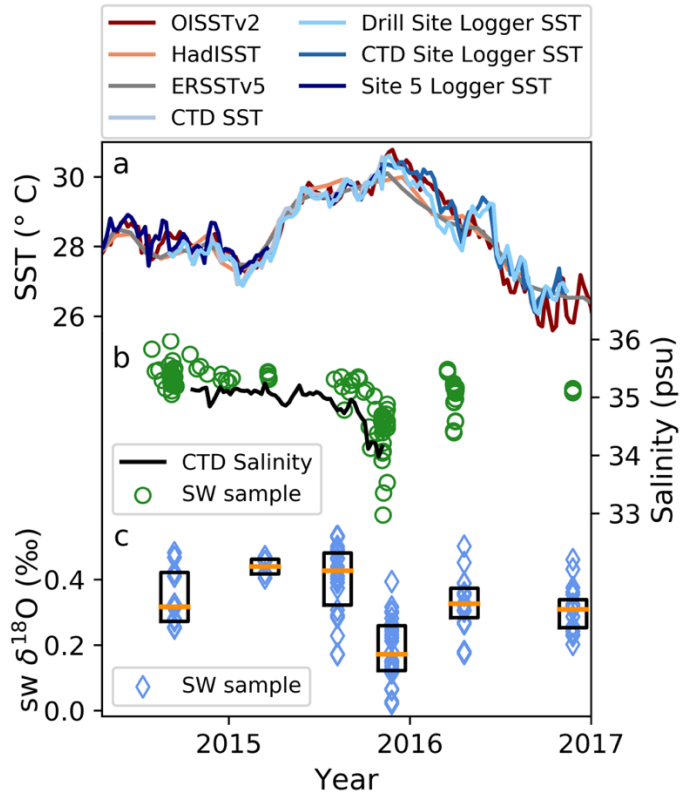
168

169 **3.2 *In situ* SST, salinity, and seawater $\delta^{18}\text{O}$ measurements**

170 We compare *in situ* SST, salinity, and $\delta^{18}\text{O}_{\text{sw}}$ from Kiritimati Island to constrain the
 171 individual contributions of SST and $\delta^{18}\text{O}_{\text{sw}}$ to coral $\delta^{18}\text{O}$ during 2015/16 El Niño event. The
 172 four *in situ* SST datasets all capture the 2015/16 El Niño event with varying coverage (Figure

173 2a). Monthly averaged *in situ* SST timeseries exhibit strong correlations with all three gridded
174 SST data products (R values of 0.90 to 0.99, Table S8). We calculate change in SST across the
175 2015/16 El Niño by subtracting the 2-year-averaged baseline SST (2013-2015) from the 3-month
176 peak of the event. Using just the Site 5 logger (which has the longest coverage across this event),
177 we calculate an increase in SST of $2.4 \pm 0.4^{\circ}\text{C}$ (1SE) at Kiritimati Island. In comparison,
178 ERSSTv5 and HadISST show similar warming of $2.4 \pm 0.4^{\circ}\text{C}$ (1SE) and $2.4 \pm 0.3^{\circ}\text{C}$ (1SE),
179 respectively, and OISSTv2 shows a slightly larger change of $2.8 \pm 0.5^{\circ}\text{C}$ (1SE).

180 To constrain the hydrological contribution to the interannual variability in the coral records,
181 we analyze *in situ* CTD salinity and salinity/ $\delta^{18}\text{O}_{\text{sw}}$ from seawater bottle samples (Figures 2b
182 and 2c). Due to the shorter duration of these timeseries, we use a 1-year baseline from mid-2014
183 to mid-2015 to calculate the change in salinity during the event. The CTD tracks a decrease in
184 salinity of 0.91 ± 0.05 psu (1SE), reaching a value of 34.14 psu during the peak of the El Niño
185 event. Salinity data from 148 seawater bottle samples show a mean decrease of 0.96 ± 0.08 psu
186 (1SE), reaching a mean value of 34.41 psu during the peak of the event. Although the absolute
187 salinity of the two data sources is offset by approximately 0.3 psu (which may be attributed to
188 differences in instrumental calibration), they capture the same relative change across the study
189 interval. Using the same time periods as the salinity calculation, the $\delta^{18}\text{O}_{\text{sw}}$ data capture a
190 decrease of $0.19 \pm 0.02\text{‰}$ (1SE), reaching a mean of 0.19‰ during the peak of the event. We
191 note that the use of a 1-year baseline here may underestimate the magnitude of the El Niño
192 anomalies, as there is less warming (and likely less freshening) from this 2014/15 baseline
193 (Figure 1). We account for this in conclusions based on this calculation.



194

195 **Figure 2.** *In situ* SST, salinity, and $\delta^{18}\text{O}_{\text{sw}}$ data spanning the 2015/16 El Niño event at Kiritimati
 196 Island. (a) Weekly SST records from 4 *in situ* temperature loggers (see Figure S1 for locations).
 197 Also plotted are weekly OISSTv2, monthly HadISSTv1.1, and monthly ERSSTv5. (b) Salinity
 198 records from the CTD (red) and seawater bottle samples (green circles). (c) Seawater $\delta^{18}\text{O}$
 199 measurements from seawater bottle samples (blue diamonds). Orange lines represent the median
 200 of the $\delta^{18}\text{O}_{\text{sw}}$ data, the boxes show the 25-75% interquartile range.

201

202 3.3 Comparison to past strong El Niño events

203 Coral $\delta^{18}\text{O}$ timeseries from Kiritimati Island show progressive depletion in mean coral $\delta^{18}\text{O}$
 204 during the peaks of the 1982/83, 1997/98, and 2015/16 strong El Niño events. Mean coral $\delta^{18}\text{O}$
 205 anomalies (3-month average centered around the peak of each event) were -5.23‰ during the

206 peak of the 1982/83 El Niño event, decreased to -5.49‰ during the 1997/98 event, and then
207 decreased to -5.59‰ during the 2015/16 event (Figure 3, Table 1). However, these El Niño are
208 superimposed on background warming and freshening trends in the tropical Pacific (Nurhati et
209 al., 2009), which produce more depleted coral $\delta^{18}\text{O}$ values over this time interval. When the
210 magnitude of each event is isolated from the mean state of the Pacific (by taking the difference
211 between the 3-month average during the peak and the 2-year baseline prior to the event; Figure
212 3), a student t-test ($p < 0.05$) shows no statistically significant difference in coral $\delta^{18}\text{O}$ magnitude
213 of these three events (Figure S3).

214 The amplitude of the 1997/98 event, both in terms of coral $\delta^{18}\text{O}$ and observed SST, is similar
215 to that of the 2015/16 event. Five out of six corals that span the 1997/98 event show similar
216 depletion in coral $\delta^{18}\text{O}$ during the peak of the 1997/98 event. The sixth coral (Nurhati-09) does
217 not fully capture SST and SSS changes across this event (Figure 3), possibly due to thermal
218 stress or sublethal bleaching (Nurhati et al., 2009). Excluding this record, the amplitude of the
219 1997/98 event is $-0.56 \pm 0.06\text{‰}$ (1SE), which is indistinguishable from the $-0.58 \pm 0.05\text{‰}$ (1SE)
220 amplitude of the 2015/2016 event. Similarly, ERSSTv5 shows statistically indistinguishable SST
221 anomalies during the 1997/98 El Niño and 2015/16 El Niño ($+2.1 \pm 0.8^\circ\text{C}$ vs $2.4 \pm 0.4^\circ\text{C}$,
222 respectively; Figure 3). Similar results are found when this calculation is performed with
223 OISSTv2 and HadISST (Figure S4, Table S8).

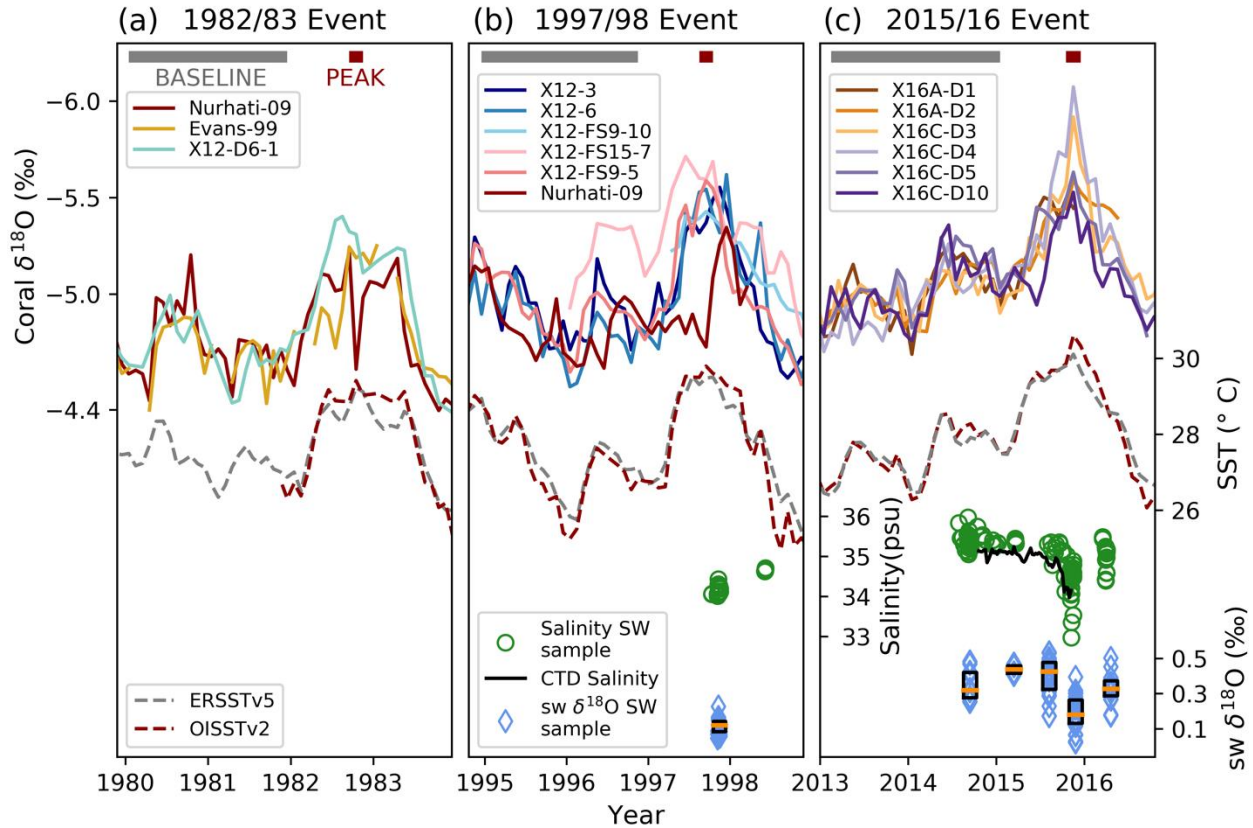
224 As limited salinity and $\delta^{18}\text{O}_{\text{sw}}$ data is available from the 1997/98 event, we only compare
225 bottle $\delta^{18}\text{O}_{\text{sw}}$ measurements from the peaks of the 1997/98 and 2015/16 events. Salinity during
226 November 1997 reached a mean of 34.17 psu, slightly lower than that of the 2015/16 event mean
227 in SW bottles (34.41 psu). Seawater $\delta^{18}\text{O}$ reached a minimum of 0.11‰ during October 1997,
228 significantly less than the 0.19‰ observed during the peak of the 2015/16 event. Thus, available

229 data show that the 1997/98 El Niño event was characterized by similar changes in coral $\delta^{18}\text{O}$ and
230 SST but slightly lower minimum salinity and seawater $\delta^{18}\text{O}$ values compared to the 2015/16
231 event.

232 For the 1982/83 event, we use two of the three coral $\delta^{18}\text{O}$ records that span this interval to
233 calculate anomalies associated with this strong El Niño, excluding the Nurhati et al., 2009 record
234 as the authors note that it does not fully capture SST and SSS changes across the peak of the
235 event. We calculate a coral $\delta^{18}\text{O}$ amplitude of $-0.52 \pm 0.05\text{‰}$ (1SE) for the 1982/83 event, which
236 is statistically indistinguishable from the 1997/98 and 2015/16 events (Figure S3). ERSSTv5
237 shows an increase of $+1.7 \pm 0.3^\circ\text{C}$ (1SE) at Kiritimati across the 1982/83 El Niño, again
238 statistically indistinguishable from SST during the 1997/98 and 2015/16 events (Figure S3) and
239 consistent with previous work (Huang et al., 2016).

240

241



242

243 **Figure 3.** Coral $\delta^{18}\text{O}$ records (solid lines) and monthly SST (dashed lines) during the (a)

244 1982/83, (b) 1997/98, and (c) 2015/16 El Niño. Horizontal bars at the top of each panel show the

245 2-year baseline (gray) and 3-month peak (red) periods used to calculate SST and coral $\delta^{18}\text{O}$ 246 anomalies for each El Niño event. Coral $\delta^{18}\text{O}$ records shown are the “X16” corals (this study),

247 “X12-3” and “X12-6” (Grothe et al., 2020), “X12-FS” fossil corals and “X12-D6-1” fossil coral

248 (Hitt et al., submitted), “Nurhati-09” (Nurhati et al., 2009), and “Evans-99” (Evans et al., 1999).

249 Coral records are plotted with offsets applied, as shown in Tables S1 and S2. Gridded SST data

250 are from ERSSTv5 and OISSTv2. Seawater $\delta^{18}\text{O}$ (open circles) and sea surface salinity (open

251 diamonds) measurements are shown where available.

252

253 **3.4 SST and hydrological contributions to coral $\delta^{18}\text{O}$**

254 To quantify the relative contributions of SST and $\delta^{18}\text{O}_{\text{sw}}$ to coral $\delta^{18}\text{O}$ during the 2015/16 El
255 Niño event, we calculated the expected temperature contribution to coral $\delta^{18}\text{O}$ using the
256 empirical relationship of $-0.2\text{‰ } ^\circ\text{C}^{-1}$ (Epstein et al., 1951), and then subtract the temperature
257 contribution from coral $\delta^{18}\text{O}$ to isolate $\delta^{18}\text{O}_{\text{sw}}$ changes (Supplement). The SST change of $+2.4 \pm$
258 0.4°C (1SE) calculated from ERSSTv5 during the 2015/16 event corresponds to an expected
259 coral $\delta^{18}\text{O}$ change of $-0.48 \pm 0.08\text{‰}$ (1SE). As the observed coral $\delta^{18}\text{O}$ change during this event
260 is $-0.58 \pm 0.05\text{‰}$ (1SE), we estimate a $\delta^{18}\text{O}_{\text{sw}}$ contribution of $-0.10 \pm 0.08\text{‰}$ (1SE), which
261 implies that $\delta^{18}\text{O}_{\text{sw}}$ accounts for $18 \pm 13\%$ (1SE) of the observed coral $\delta^{18}\text{O}$ change during the
262 2015/16 event, with SST contributing to the remaining $82 \pm 13\%$ (1SE ; Table 1 and S4). We
263 find similar results when repeating this calculation with OISSTv2 and HadISST (Tables S5-S8).
264 We note that SST uncertainty dominates this calculation, and a full propagation of the 2SE
265 uncertainties through SST, coral $\delta^{18}\text{O}$, and $\delta^{18}\text{O}_{\text{sw}}$ would likely double the range of permissible
266 percentages.

267 The *in situ* $\delta^{18}\text{O}_{\text{sw}}$ measurements provide a powerful additional constraint on the coral $\delta^{18}\text{O}$
268 budget, given the weak constraints afforded by SST and coral $\delta^{18}\text{O}$ observations outlined above.
269 Given the observed change in $\delta^{18}\text{O}_{\text{sw}}$ of $-0.19 \pm 0.02\text{‰}$ (1SE) during the peak of the 2015/16 El
270 Niño, the $\delta^{18}\text{O}_{\text{sw}}$ contribution is constrained to $\sim 30\text{-}35\%$ (including all values that fall within the
271 1 SE uncertainty range; Tables 1, S4, Figure S5). These values do not change if different SST
272 products are used (Tables S5, S6), and are relatively insensitive to the choice of 1-year versus 2-
273 year baselines for the calculations of anomalies (Table S7).

274 Using the same approach, we calculate the SST and $\delta^{18}\text{O}_{\text{sw}}$ contributions to coral $\delta^{18}\text{O}$
275 changes across the 1997/98 and 1982/83 El Niño events (Tables 1, S5), although the lack of
276 observed $\delta^{18}\text{O}_{\text{sw}}$ data translates to large uncertainties in these estimates. For the 1997/98 event,

277 we find a hydrological contribution of approximately $26 \pm 28\%$ (1SE), which is similar in mean
 278 but associated with larger uncertainty. For the 1982/83 event, we find a $\delta^{18}\text{O}_{\text{sw}}$ contribution of 34
 279 $\pm 13\%$ (1SE). In short, we find consistent relative contributions from SST and $\delta^{18}\text{O}_{\text{sw}}$ anomalies
 280 (roughly 70% and 30%, respectively) to coral $\delta^{18}\text{O}$ anomalies across the three strong El Niño
 281 events in question.

282

283 **Table 1.** Comparison of SST (from ERSSTv5) and estimated $\delta^{18}\text{O}_{\text{sw}}$ contributions to observed
 284 coral $\delta^{18}\text{O}$ anomalies associated with strong El Niño events at Kiritimati Island. Changes are
 285 calculated as the 3-month peak of the event minus a 2-year baseline, reported with 1SE
 286 uncertainties (Supplement, Table S4). For the 2015/16 event, observed changes in $\delta^{18}\text{O}_{\text{sw}}$ and
 287 associated contributions are also shown, with 1SE uncertainty, calculating using the available 1-
 288 year baseline.

		1982/83 Event	1997/98 Event	2015/16 Event
<i>A</i>	Observed peak mean coral $\delta^{18}\text{O}$	$-5.23 \pm 0.07 \text{ ‰}$	$-5.49 \pm 0.10 \text{ ‰}$	$-5.59 \pm 0.05 \text{ ‰}$
<i>B</i>	Observed Δ coral $\delta^{18}\text{O}$	$-0.52 \pm 0.05 \text{ ‰}$	$-0.56 \pm 0.06 \text{ ‰}$	$-0.58 \pm 0.05 \text{ ‰}$
<i>C</i>	Observed Δ SST (ERSSTv5)	$+1.7 \pm 0.3 \text{ °C}$	$+2.1 \pm 0.8 \text{ °C}$	$+2.4 \pm 0.4 \text{ °C}$
<i>D</i>	Estimated SST-driven Δ coral $\delta^{18}\text{O}$ ($C \times 0.2 \text{ ‰ °C}^{-1}$)	$-0.35 \pm 0.07 \text{ ‰}$	$-0.42 \pm 0.16 \text{ ‰}$	$-0.48 \pm 0.08 \text{ ‰}$
<i>E</i>	Estimated Δ sw $\delta^{18}\text{O}$ ($B - D$)	$-0.18 \pm 0.07 \text{ ‰}$	$-0.14 \pm 0.15 \text{ ‰}$	$-0.10 \pm 0.08 \text{ ‰}$
<i>F</i>	Observed Δ sw $\delta^{18}\text{O}$ (SW bottle samples)	N/A	N/A	$-0.19 \pm 0.02 \text{ ‰}$
<i>G</i>	Estimated sw $\delta^{18}\text{O}$ contribution ($E/B \times 100$)	$34 \pm 13 \text{ ‰}$	$26 \pm 28 \text{ ‰}$	$18 \pm 13 \text{ ‰}$
<i>H</i>	Observed sw $\delta^{18}\text{O}$ contribution ($F/B * 100$)	N/A	N/A	$33 \pm 4 \text{ ‰}$

289

290 4 Discussion and Conclusions

291 Our analysis of Kiritimati coral records demonstrates that corals $\delta^{18}\text{O}$ at this site faithfully
292 record SST and hydrological anomalies associated with the strongest El Niño events. Paired *in*
293 *situ* temperature, seawater $\delta^{18}\text{O}$, and coral $\delta^{18}\text{O}$ confirm that all six cores collected in 2016
294 accurately capture the SST and $\delta^{18}\text{O}_{\text{sw}}$ changes observed during the 2015/2016 El Niño event,
295 within uncertainties (Figure S5). We observe no evidence of hiatuses in x-rays of our cores
296 (Figure S6), such as those found in Galapagos coral during strong El Niños (Dunbar et al., 1994,
297 Jimenez et al., 2018), nor do we observe any signs of thermal stress in our coral $\delta^{18}\text{O}$ data (e.g.,
298 Hetzinger et al., 2016). However, we observe the largest variance in coral $\delta^{18}\text{O}$ during peak El
299 Niño warming, which could bias studies of past El Niño amplitudes based on single coral $\delta^{18}\text{O}$
300 records. Nurhati et al., 2009 hypothesized that the attenuated signal of the 1997/98 El Niño event
301 in their Kiritimati coral $\delta^{18}\text{O}$ records may have resulted from a reduced precipitation or a growth
302 hiatus. Alternatively, high coral $\delta^{18}\text{O}$ variance during peak El Niño conditions may reflect more
303 meter-scale variance in temperature and seawater $\delta^{18}\text{O}$ during El Niño extremes, given the strong
304 gradients that occur at this time between the surface and depth, and between the lagoon and the
305 open ocean, during a prolonged period of reduced wind-driven mixing.

306 Our investigation of the relative contributions of SST and $\delta^{18}\text{O}_{\text{sw}}$ anomalies to Kiritimati
307 coral $\delta^{18}\text{O}$ anomalies across the 2015/16 El Niño event shows that SST conditions are
308 responsible for ~70% of the coral $\delta^{18}\text{O}$ signal. Similar estimates for SST contributions to
309 Kiritimati coral $\delta^{18}\text{O}$ records spanning the 1982/83 and 1997/98 El Niño events (mean values of
310 66 ± 13 and $74 \pm 28\%$, respectively) bolsters our confidence in our findings from the 2015/16 El
311 Niño event, although these estimates are associated with much larger uncertainties given the lack

312 of *in situ* $\delta^{18}\text{O}_{\text{sw}}$ observations. Our findings are consistent with isotope-enabled climate model
313 studies (Russon et al., 2013) which found an upper bound of 75% for the SST contribution to
314 Kiritimati coral $\delta^{18}\text{O}$, as well as with previous empirically derived estimates (e.g., McGregor et
315 al., 2011).

316 When placed within the context of centuries worth of coral $\delta^{18}\text{O}$ data from Kiritimati Island
317 and nearby sites, our results provide key constraints on the physical drivers of the recent
318 intensification of interannual coral $\delta^{18}\text{O}$ variability in central tropical Pacific corals (Grothe et
319 al., 2020). Given that our results show a ~30% contribution from $\delta^{18}\text{O}_{\text{sw}}$ to the coral $\delta^{18}\text{O}$
320 anomalies during the three largest El Niño events in recent decades, it is unlikely that the
321 observed ~25% increase in interannual coral $\delta^{18}\text{O}$ variability in recent decades relative to the
322 past millennia (Grothe et al., 2020) is caused exclusively by an amplification of the hydrologic
323 response to ENSO-related SST anomalies. Furthermore, instrumental climate data indicate that
324 regional freshening is dynamically linked to warm SST anomalies during El Niño events in this
325 location (Ropelewski and Halpert, 1987), suggesting that the observed increase in coral $\delta^{18}\text{O}$
326 variability is driven by an increase in both temperature and hydrological variability.

327 Our data support the fidelity of Kiritimati coral $\delta^{18}\text{O}$ records for long-term ENSO
328 reconstruction, even under extreme temperature stress associated with a very strong El Niño
329 event. Taken together, the coral $\delta^{18}\text{O}$ records, *in situ* SST, and $\delta^{18}\text{O}_{\text{sw}}$ data analyzed here show
330 that SST dominates the ENSO-related coral $\delta^{18}\text{O}$ signal (~70%), with a smaller influence from
331 $\delta^{18}\text{O}_{\text{sw}}$ (~30%). Such quantitative constraints are made possible by *in situ* seawater $\delta^{18}\text{O}$
332 observations collected across the event, demonstrating the value of prioritizing *in situ* seawater
333 $\delta^{18}\text{O}$ observations in the design of regional to global-scale ocean observing systems, including
334 TPOS2020 (Kessler et al., 2019). Calibration studies such as these are necessary to better

335 understand the ENSO signals captured in coral $\delta^{18}\text{O}$ records and provide insight on signals
336 captured by coral records over longer timescales. Our results suggest that a documented increase
337 in interannual coral $\delta^{18}\text{O}$ variability at the site from the preindustrial to the present (Grothe et al.,
338 2020) likely reflects an increase in ENSO-related SST.

339 **5 Acknowledgments, Samples, and Data**

340 We acknowledge the Republic of Kiribati for granting us permits to collect samples and conduct
341 research on Kiritimati Island (number 005/13), provided by the Environment and Conservation
342 Division. We especially thank Tiito Teabi for his support and expertise in the field on numerous
343 expeditions to Kiritimati from 2012 to 2016. This research was funded by National Science
344 Foundation Awards 1502832, 1658182, 1635068, 1836645, to K.M.C, 1446343 to S.S., 1446274
345 to J.K.B., and 9802056 (Moana Wave Cruise). Additional funding from a Georgia Tech
346 Presidential Undergraduate Research Award and a National Science Foundation Graduate
347 Research Fellowship was used to support G.K.O. All data and metadata are archived at NCDC
348 (<https://www.ncdc.noaa.gov/paleo-search/study/28291>) and have registered International Geo
349 Sample Numbers IECXI000B, IECXI000C, IECXI000D, IECXI000E, IECXI000F, and
350 IECXI000G (i.e., [igsn.org/IECXI000B](https://www.igsn.org/IECXI000B)).

351

352 **References**

- 353 1. Bellenger, H., Guilyardi, E., Leloup, J., Lengaigne, M., & Vialard, J. (2014). ENSO
354 representation in climate models: from CMIP3 to CMIP5. *Climate Dynamics*, 42(7-8),
355 1999-2018. <https://doi.org/10.1007/s00382-013-1783-z>
- 356 2. Bonfils, C. J. W., Santer, B. D., Phillips, T. J., Marvel, K., Leung, L. R., Doutriaux, C., &
357 Capotondi, A. (2015). Relative contributions of mean-state shifts and ENSO-driven

- 358 variability to precipitation changes in a warming climate. *Journal of Climate*, 28(24),
359 9997-10013. <https://doi.org/10.1175/JCLI-D-15-0341.1>
- 360 3. Brown, J. R., Brierley, C. M., An, S.-I., Guarino, M., Stevenson, S., Williams, C. J. R., et
361 al. (2020). Comparison of past and future simulations of ENSO in CMIP5/PMIP3 and
362 CMIP6/PMIP4 models. *Climate of the Past*, 16, 1777-1805. [https://doi.org/10.5194/cp-](https://doi.org/10.5194/cp-16-1777-2020)
363 [16-1777-2020](https://doi.org/10.5194/cp-16-1777-2020)
- 364 4. Cai, W., Borlace, S., Lengaigne, M., van Rensch, P., Collins, M., Vecchi, G., et al.
365 (2014). Increasing frequency of extreme El Niño events due to greenhouse warming.
366 *Nature Climate Change*, 4, 111-116. <https://doi.org/10.1038/nclimate2100>
- 367 5. Cai, W., Santoso, A., Wang, G., Yeh, S.-W., An, S.-I., Cobb, K. M., et al. (2015). ENSO
368 and greenhouse warming. *Nature Climate Change*, 5, 849-859.
369 <https://doi.org/10.1038/nclimate2743>
- 370 6. Carilli, J. E., Hartmann, A. C., Heron, S. F., Pandolfi, J. M., Cobb, K.M., Sayani, H. S., et
371 al. (2017). *Limnology and Oceanography*, 62(6), 2850-2863.
372 <https://doi.org/10.1002/lno.10670>
- 373 7. Claar, D. C., Cobb, K. M., Baum, J. K. (2019). In situ and remotely sensed temperature
374 comparison on a Central Pacific atoll. *Coral Reefs*, 38(6), 1343-1349.
375 <https://doi.org/10.1007/s00338-019-01850-4>
- 376 8. Cobb, K. M., Charles, C. D., & Hunter, D. E. (2001). A central tropical Pacific coral
377 demonstrates Pacific, Indian, and Atlantic decadal climate connections. *Geophysical*
378 *Research Letters*, 28(11), 2209–2212. <https://doi.org/10.1029/2001GL012919>
- 379 9. Cobb, K. M. (2002). Thesis, University of California, San Diego.

- 380 10. Cobb, K. M., Charles, C. D., Cheng, H., & Edwards, R. L. (2003). El Niño/Southern
381 Oscillation and tropical Pacific climate during the last millennium. *Nature*, 424, 271.
382 <https://doi.org/10.1038/nature01779>
- 383 11. Cobb, K. M., Westphal, N., Sayani, H. R., Watson, J. T., Di Lorenzo, E., Cheng, H., et al.
384 (2013). Highly Variable El Niño–Southern Oscillation Throughout the Holocene.
385 *Science*, 339(6115), 67-70. <https://doi.org/10.1126/science.1228246>
- 386 12. Conroy, J. L., Cobb, K. M., Lynch-Stieglitz, J., & Polissar, P. J. (2014). Constraints on
387 the salinity–oxygen isotope relationship in the central tropical Pacific Ocean, *Marine*
388 *Chemistry*, 161, 26–33. <https://doi.org/10.1016/j.marchem.2014.02.001>
- 389 13. Dunbar, R. B., Wellington, G. W., Colgan, M. W., & Glynn, P.W. (1994). Eastern Pacific
390 sea surface temperature since 1600 AD: the $\delta^{18}\text{O}$ record of climate variability in
391 Galapagos corals. *Paleoceanography*, 9(2), 291-315. <https://doi.org/10.1029/93PA03501>
- 392 14. Epstein, S., Buchsbaum, R., Lowenstam, H., & Urey, H. (1951). Carbonate-water
393 isotopic temperature scale. *Geological Society of America Bulletin*, 62(4), 417-426.
394 [https://doi.org/10.1130/0016-7606\(1951\)62\[417:CITS\]2.0.CO;2](https://doi.org/10.1130/0016-7606(1951)62[417:CITS]2.0.CO;2)
- 395 15. Evans, M. N., Fairbanks, R. G., & Rubenstone, J. L. (1999). The thermal oceanographic
396 signal of El Niño reconstructed from a Kiritimati Island coral. *Journal of Geophysical*
397 *Research: Oceans*, 104(C6), 13409–13421. <https://doi.org/10.1029/1999JC900001>
- 398 16. Fairbanks, R. G., Evans, M. N., Rubenstone, J. L., Mortlock, R. A., Broad, K., Moore,
399 M.D., & Charles, C.D. (1997). Evaluating climate indices and their geochemical proxies
400 measured in corals, *Coral Reefs*, 16, S93–S100. <https://doi.org/10.1007/s003380050245>
- 401 17. Freund, M. B., Henley, B. J., Karoly, D. J., McGregor, H. V., Abram, N. J., &
402 Dommenget, D. (2019). Higher frequency of Central Pacific El Niño events in recent

- 403 decades relative to past centuries. *Nature Geoscience*, 12, 450-455.
404 <https://doi.org/10.1038/s41561-019-0353-3>
- 405 18. Grothe, P. R., Cobb, K. M., Liguori, G., Di Lorenzo, E., Capotondi, A., Lu, Y., et al.
406 (2020). Enhanced El Niño-Southern Oscillation variability in recent decades.
407 *Geophysical Research Letters*, 47(7), e2019GL083906.
408 <https://doi.org/10.1029/2019GL083906>
- 409 19. Hetzinger, S., Pfeiffer, M., Dullo, W., Zinke, J., & Garbe-Schonberg, D. (2016). A
410 change in coral extension rates and stable isotopes after El Niño-induced coral bleaching
411 and regional stress events. *Scientific Reports*, 6, 32879. <https://doi.org/10.1038/srep32879>
- 412 20. Hitt, N. T., Sayani, H. R., Atwood, A. R., Grothe, P. R., Maupin, C., Ellis, S., et al.
413 (submitted). Central equatorial Pacific warming and freshening in the 20th century: New
414 insights from a coral ensemble approach. *Geophysical Research Letters*.
- 415 21. Huang, B., Thorne, P. W., Banzon, V. F., Boyer, T., Chepurin, G., Lawrimore, J. H., et
416 Al. (2017). Extended Reconstructed Sea Surface Temperature version 5 (ERSSTv5),
417 Upgrades, validations, and intercomparisons. *Journal of Climate*, 30(20), 8179-8205.
418 <https://doi.org/10.1175/JCLI-D-16-0836.1>
- 419 22. Jimenez, G. Cole, J. E., Thompson, D. M., Tudhope, A. W. (2018). Northern Galapagos
420 corals reveal twentieth century warming in the eastern tropical Pacific. *Geophysical*
421 *Research Letters*, 45(4), 1981-1988. <https://doi.org/10.1002/2017GL075323>
- 422 23. Kessler, W. S., Wijffels, S. E., Cravatte, S., Smith, N., & Lead Authors. (2019) Second
423 Report of TPOS 2020. GOOS-234.

- 424 24. Li, J., Xie, S.-P., Cook, E. R., Morales, M. S., Christie, D. A., Johnson, N. C., et al.
425 (2013). El Niño modulations over the past seven centuries. *Nature Climate Change*, 3,
426 822-826. <https://doi.org/10.1038/nclimate1936>
- 427 25. Liu, Y., Cobb, K. M., Song, H., Li, Q., Li, C.-Y., Nakatsuka, T., et al. (2017). Recent
428 enhancement of central Pacific El Niño variability relative to last eight centuries. *Nature*
429 *Communications*, 8, 15386. <https://doi.org/10.1038/ncomms15386>
- 430 26. McGregor, S., Timmermann, A., England, M. H., Elison Timm, O., & Wittenberg, A. T.
431 (2013). Inferred changes in El Niño–Southern Oscillation variance over the past six
432 centuries. *Climate of the Past*, 9(5), 2269–2284. <https://doi.org/10.5194/cp-9-2269-2013>
- 433 27. Ng, B., Cai, W., Cowan, T. & Bi, D. (2021). Impacts of low-frequency internal climate
434 variability and greenhouse warming on El Niño- Southern Oscillation. *Journal of*
435 *Climate*, 34(6), 2205-2218. <https://doi.org/10.1175/JCLI-D-20-0232.1>
- 436 28. Nurhati, I. S., Cobb, K. M., Charles, C. D., & Dunbar, R. B. (2009). Late 20th century
437 warming and freshening in the central tropical Pacific. *Geophysical Research Letters*,
438 36(21), L21606. <https://doi.org/10.1029/2009GL040270>
- 439 29. Nurhati, I. S., Cobb, K. M., & Di Lorenzo, E. (2011). Decadal-scale SST and salinity
440 variations in the central tropical Pacific: signatures of natural and anthropogenic climate
441 change. *Journal of Climate*, 24(13), 3294-3308. <https://doi.org/10.1175/2011JCLI3852.1>
- 442 30. Power, S., Delage, F., Chung, C., Kociuba, G., & Keay, K. (2013). Robust twenty-first-
443 century projections of El Niño and related precipitation variability. *Nature*, 502, 541-545.
444 <https://doi.org/10.1038/nature12580>
- 445 31. Rayner, N. A., Parker, D. E., Horton, E. B., Folland, C. K., Alexander, L. V., Rowell, D.
446 P., et al. (2003). Global analyses of sea surface temperature, sea ice, and night marine air

- 447 temperature since the late nineteenth century *Journal of Geophysical Research:*
448 *Atmospheres*, 108(D14), 4407. <https://doi.org/10.1029/2002JD002670>
- 449 32. Reynolds, R. W., Rayner, N. A., Smith, T. M., Stokes, D. C., & Wang, W. (2002). An
450 Improved in situ and satellite SST analysis for climate. *Journal of Climate*, 15(13), 1609–
451 1625. [https://doi.org/10.1175/1520-0442\(2002\)015<1609:AIISAS>2.0.CO;2](https://doi.org/10.1175/1520-0442(2002)015<1609:AIISAS>2.0.CO;2)
- 452 33. Ropelewski, C. F., and Halpert, M. S. (1987). Global and regional scale precipitation
453 patterns associated with the El Niño/Southern Oscillation. *Monthly Weather Review*,
454 115(7), 1606-1626. [https://doi.org/10.1175/1520-0493\(1987\)115%3C1606:GARSPP%3E2.0.CO;2](https://doi.org/10.1175/1520-0493(1987)115%3C1606:GARSPP%3E2.0.CO;2)
- 455
- 456 34. Russon, T., Tudhope, A. W., Hegerl, G. C., Collins, M., & Tindall, J. (2013). Inter-
457 annual tropical Pacific climate variability in isotope-enabled CGCM: implications for
458 interpreting coral stable oxygen isotope records of ENSO. *Climate of the Past*, 9(4),
459 1542-1557. <https://doi.org/10.5194/cp-9-1543-2013>
- 460 35. Sayani, H. R., Cobb, K. M., DeLong, K., Hitt, N. T., & Druffel, E. R. M. (2019).
461 Intercolony $\delta^{18}\text{O}$ and Sr/Ca variability among *Porites* spp. corals at Palmyra Atoll:
462 Toward more robust coral-based estimates of climate. *Geochemistry, Geophysics,*
463 *Geosystems*, 20(11), 5270-5284. <https://doi.org/10.1029/2019GC008420>
- 464 36. Stevenson, S. L. (2012). Significant changes to ENSO strength and impacts in the
465 twenty-first century: Results from CMIP5. *Geophysical Research Letters*, 39(17),
466 L17703. <https://doi.org/10.1029/2012GL052759>
- 467 37. Stevenson, S., Wittenberg, A. T., Fasullo, J., Coats, S., & Otto-Bliesner, B. (2021).
468 Understanding Diverse Model Projections of Future Extreme El Niño. *Journal of*
469 *Climate*, 34(2), 449-464. <https://doi.org/10.1175/JCLI-D-19-0969.1>

- 470 38. Wang, B., Luo, X., Yang, Y., Sun, W., Cane, M. A., Cai, W., et al. (2019). Historical
471 change of El Niño properties sheds light on future changes of extreme El Niño.
472 *Proceeding of the National Academy of Sciences*, 116(45), 22512-22517.
473 <https://doi.org/10.1073/pnas.1911130116>